

DOI: 10.71762/T6MG-6N32

Research Paper

Finding the Elastic Modules Using Nanoindentation by Atomic Force Microscope by Considering 5 Different Types of Polymers

Iraj Rezaei1*

¹Department of Mechanic, ET.C., Islamic Azad University, Tehran, Iran *Email of the Corresponding Author: 0071359044@iau.ac.ir Received: August 9, 2025; Revised: September 28, 2025; Accepted: October 13, 2025

Abstract

In this research, the elastic modules of five different types of polymers, used as soft samples, have been investigated using nanoindentation by atomic force microscopy. Initially, the elastic modulus of the polymers was obtained using the NT-MDT SOLVER P47 scanning probe microscope for both extension and retraction strokes. Considering the importance of the subject and its application in the industry. After making macropolymers, their elastic modulus and adhesion force have been obtained for both penetration and return modes of the microscope. To investigate the mechanical properties of macropolymers, a GPK atomic force microscope model, NanoWizard 3, along with its specialized software, version 0.5.96, was used. In this research, Young's modulus was expressed for all specimens using nanoindentation and tensile testing techniques. The outcomes display that a decrease in Young's modulus increases the diversity among the Young's modulus resulting from nanoindentation and tensile testing techniques. By increasing the Young's modulus, the changes in the elastic modulus resulting from the extension and retraction regimes were reduced.

Keywords

Atomic Force Microscope, Macro Polymer, Elastic Modulus

1. Introduction

In 1983, IBM scientists Roher, Binning, Gerber, and Weibel [1] invented a powerful device for studying the surface samples. This powerful device was a Scanning Tunneling Microscope (STM). In the scanning tunneling microscope, a metallic tip scans the sample. The tip is mechanically connected to the scanner, an XYZ positioning device realized using piezoelectric materials [2]. The sample is biased positively or negatively, allowing a small current, known as the "tunneling current", to flow when the tip is in contact with the sample [3]. This tunneling current is amplified and measured. With the help of the tunneling current, the feedback electronics maintain a constant distance between the tip and the sample. If the tunneling current exceeds its preset value, the distance between the tip and the sample is increased; if it falls below this value, the feedback decreases the distance. The tip scans the sample surface line by line, following its topography. The tunneling current flows across the small gap that separates the tip from the sample. In fact, minimal changes in the tip-sample separation induce significant changes in the tunneling current, allowing the tip-sample

separation to be controlled with great precision [4]. The disadvantage of STM is that it can only be applied to conductive materials; thus, insulating materials cannot be imaged by STM [5].

2. Definition of Polymeric Samples Using AFM Approach and Tensile Testing

The elastic modules of polymers, including Polystyrene (PS), polypropylene (PP), polycarbonate (PC), acrylonitrile butadiene styrene (ABS), and high-impact polystyrene (HIPS), were obtained by applying two different methods

2.1. Elasticity Behavior Simulation

By supposing δ and $\acute{\delta}$ as the movement of the piezoelectric part and tip, respectively, and dependence of $\acute{\delta}$ to the electrical signal D, for each contact location [6]:

$$\delta = A(D - D_0) \tag{1}$$

A is the cantilever sensitivity and D_0 is the initial cantilever deviation signal. By supposing P as the used force and Λ as the tip-specimen stiffness and k as the beam stiffness:

$$P = k\delta = \Lambda(\delta - \delta_0) \tag{2}$$

From the equations (1) and (2), it may be concluded that:

$$\delta = A(D - D_0) \left(1 + \frac{k}{4} \right) \tag{3}$$

The Sneddon's contact principle is used [7]:

$$\Lambda = 2E_r a \tag{4}$$

a and E_r are introduced as the radius and reduced Young's modulus of the tip-specimen interaction.

$$\frac{1}{E_r} = \frac{1 - \nu_S^2}{E_S} + \frac{1 - \nu_{tip}^2}{E_{tip}} \tag{5}$$

 E_s and E_{tip} are related to the specimen and tip respectively. Applying equations (3) and (4), it is concluded:

$$K = A\left(1 + \frac{k}{1 + 2E_r a}\right) \tag{6}$$

$$\delta = K(D - D_0) \tag{7}$$

For calibration, two arbitrary specimens with known Young's modulus should be used. Variables A and a, as two unknown variables, can be calculated. By identifying these variables, it is possible to estimate the Young's modulus of every specimen (Figure 1) [8].

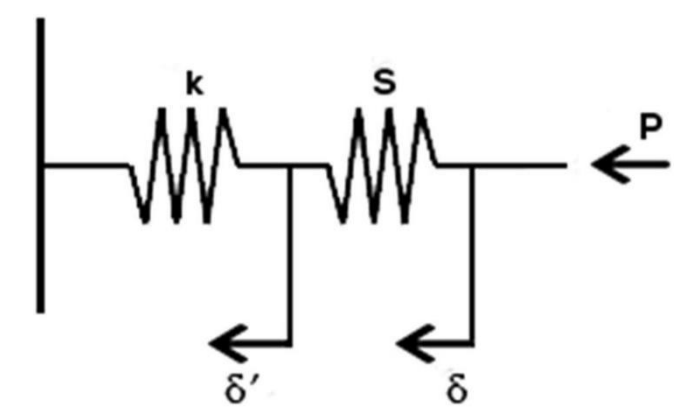


Figure 1. Contact model of the elastic bending for beam with the specimen

3. Experimental Method

All the polymeric powders purchased from Tabriz Petrochemical Company are used to produce suitable ingots. To produce the ingots, the hot press process was used. Dr. Collin GMBH (Press P400, D-85560) was used to form the powders.

4. Defining of Elastic Modules Using Tensile Test Method

The polymer ingot dimension was $20 \times 20 \times 0.3$ cm for the tensile test method. After making the polymer ingots, a computer numerical control (CNC) machine (Mori Seiki Co., Ltd., Nara, Japan, MV-junior model) was used to generate the macro models (Figure 2a) for tensile testing to obtain the macro-Young's modulus. The tensile testing was performed using a tensile testing machine and the ISO 527-0 method (Santam STM-150) (Figure 2b).

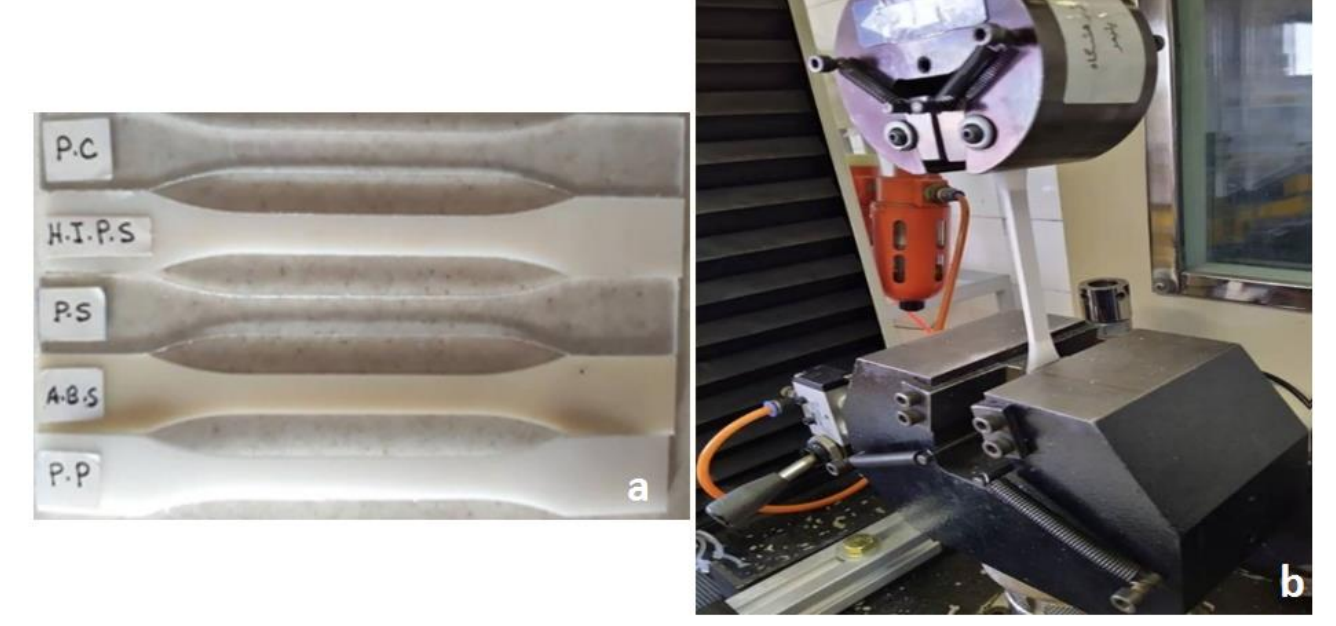


Figure 2. a) Macro polymer models b) Tensile testing machine (Santam STM-150)

5. Finding the Elastic Modules Using Nanoindentation by AFM

To determine the elastic modules of polymers using AFM, test sheets with dimensions of $2\times2\times0.3$ cm were produced. These sheets were then polished with silicon carbide and diamond to achieve smooth surfaces suitable for AFM. Figures 3 and 4 show the NT-MDT SOLVER P47 AFM with the MIKROMASCH HQNSC15 AFM probe, respectively. The mechanical specifications for the beam are: Young's modulus 1.5×1011 Pa, length $130~\mu m$, width $37~\mu m$, thickness $3.59~\mu m$, density $\rho=3270 kg/m^3$, cantilever stiffness 29.22~N/m and tip height H=15 μ m Poly ethylene (PE) with 326.69×106 Pa as Young's modulus and EPDM with Young's modulus 5.43×106 Pa were chosen as the two reversion specimens to calibrate.

The red graphs represent the extent of the regime, and the blue lines display the retraction. Based on the hysteresis between two strokes, the adhesion is produced. Applying EPDM rubber and polyethylene for calibration, A as the beam sensitivity is 72.98 nm/nA and 83.67 nm/nA for extension and retraction strokes, respectively. K, as the slope for the contact, will be 78.35 nm/nA and 89.558 nm/nA for extend and retract strokes, respectively. From the graphs, it can be seen that increasing the Young's modulus reduces the slope of the contact.

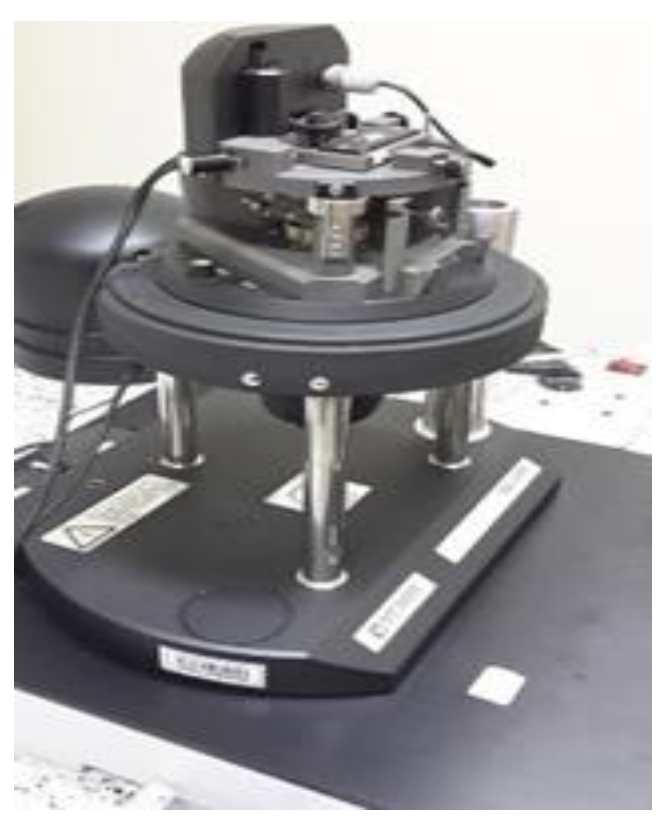


Figure 3. NT-MDT SOLVER P47 scanning probe microscope



Figure 4. MIKROMASCH HQNSC15 AFM probe

Figures 5 to 9 display the vertical displacement of the AFM cantilever against the piezoelectric displacement for twenty specimens. The red graphs represent the extent of the regime, and the blue lines display the retraction. Based on the hysteresis between two strokes, the adhesion is produced. Applying EPDM rubber and polyethylene for calibration, display the vertical displacement of the AFM cantilever against the piezoelectric displacement for twenty points for the specimens.

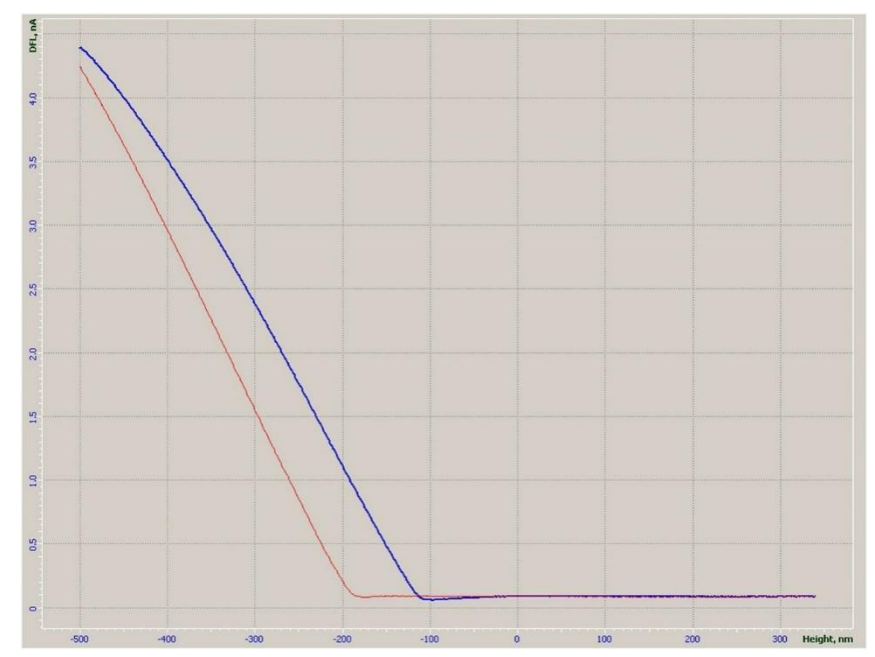


Figure 5. Average vertical deflection of the AFM cantilever versus (piezoelectric) movement for 20 indents for polystyrene (PS) sample by NT-MDT SOLVER P47 scanning probe microscope

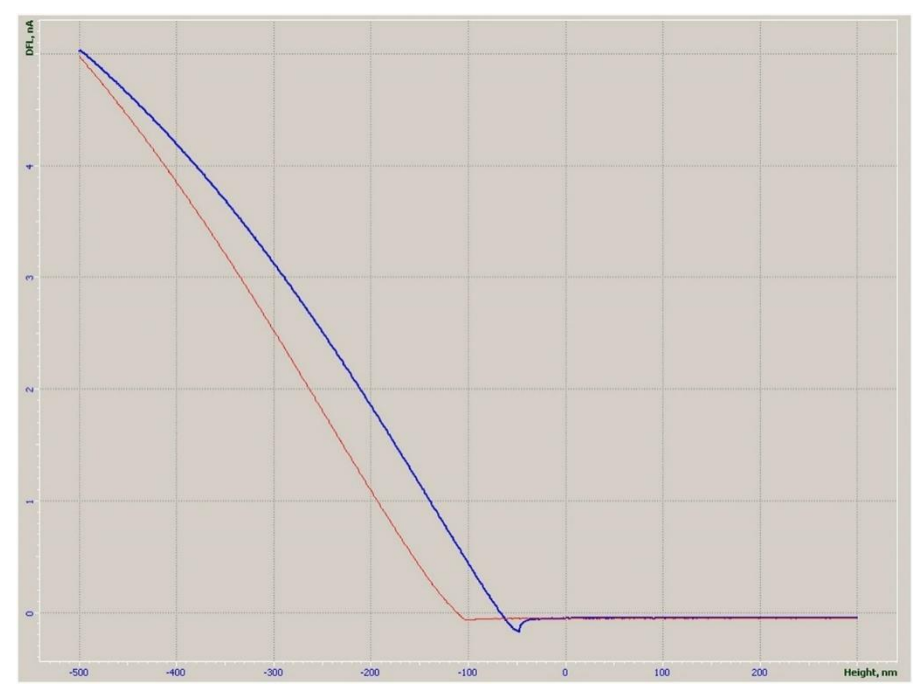


Figure 6. Average vertical deflection of the AFM cantilever versus (piezoelectric) movement for 20 indents for polypropylene (PP) sample by NT-MDT SOLVER P47 scanning probe microscope

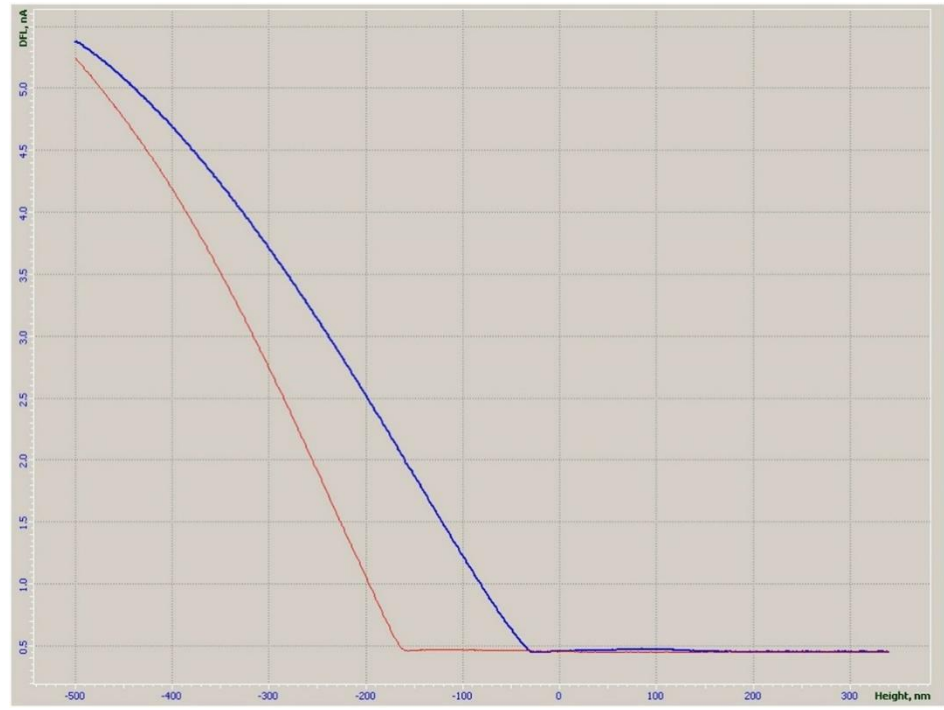


Figure 7. Average vertical deflection of the AFM cantilever versus (piezoelectric) movement for 20 indents for polycarbonate (PC) sample by NT-MDT SOLVER P47 scanning probe microscope

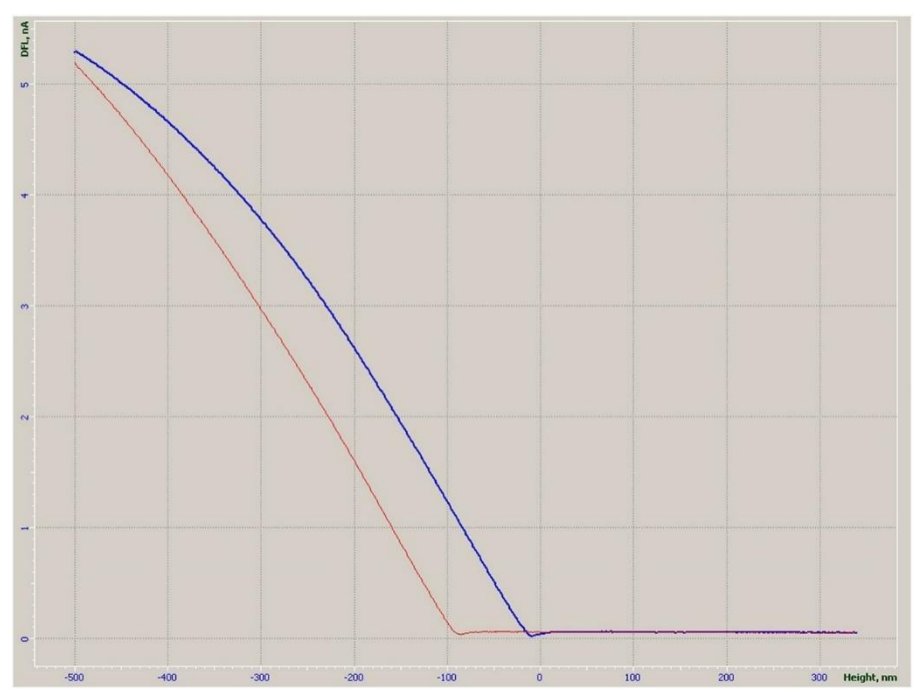


Figure 8. Average vertical deflection of the AFM cantilever versus (piezoelectric) movement for 20 indents for acrylonitrile butadiene styrene (ABS) sample by NT-MDT SOLVER P47 scanning probe microscope

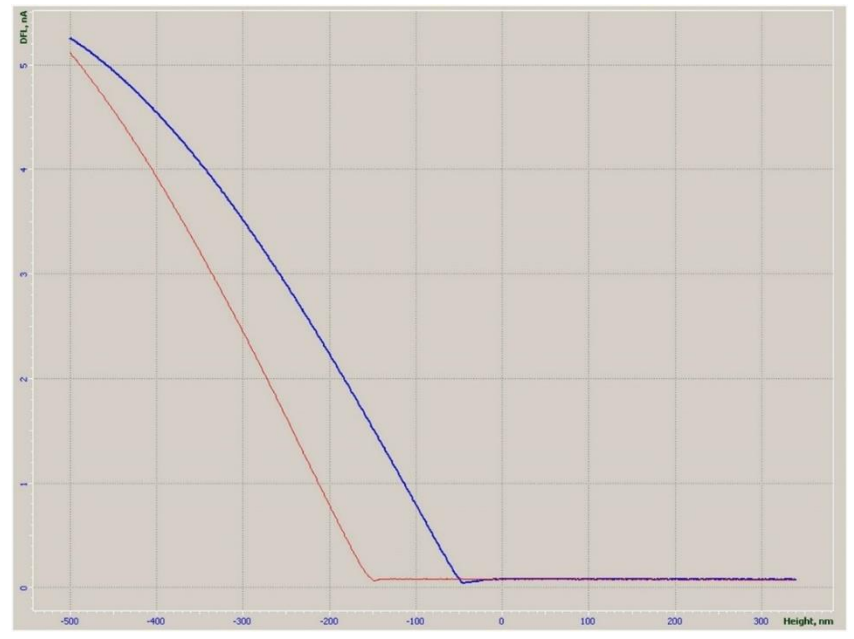


Figure 9. Average vertical deflection of the AFM cantilever versus (piezoelectric) movement for 20 indents for highimpact polystyrene (HIPS) sample by NT-MDT SOLVER P47 scanning probe microscope

Table 1 displays the Young's modulus for all the presented polymeric specimens. Young's modulus is expressed for all specimens using nanoindentation and tensile testing techniques. The outcomes display that a decrease in Young's modulus increases the diversity among the Young's modules resulting from nanoindentation and tensile testing techniques. By increasing the Young's modulus, the changes in the elastic modulus resulting from the extension and retraction regimes were reduced.

Table 1. Elastic modules for the specimens by nanoindentation and tensile testing techniques

Specimen	Young's modulus (nanoindentation) (Pa) extend strokes	Young's modulus (nanoindentati on) (Pa) retract strokes	K nm/nA extend strokes	Diversit y (%) retract strokes	K nm/nA retract strokes
Poly ethylene (PE)	-	-	78.35	-	89.558
EPDM rubber	-	-	344.338	-	381.172
Poly styrene (PS)	2.46×10^{9}	1.99×10^{9}	73.71	32.5	84.65
Poly propylene (PP)	1.12×10^9	9.04×10^8	74.56	39.73	85.80
Poly carbonate (PC)	1.81×10^9	1.46×10^9	73.94	37.6	84.97
Acrylonitrile butadiene styrene (ABS)	2.014×10^9	1.62×10^9	73.87	35.2	84.87
High impact ploy styrene (HIPS)	1.26×10^9	1.01×10^9	74.41	38.7	85.58

6. Results

In this section, the amplitude of frequency response functions for vertical and rotational displacements, as well as resonant frequencies, of the first to third vibrational modes in culture media have been obtained. To achieve maximum accuracy, all relevant details have been carefully considered and taken into account. In the current study, the effects of the presence and absence of tip-sample interaction force in air and water as the surroundings, the viscosity of liquids as environments, the cantilever length, and the cantilever breadth and thickness on the amplitude of frequency response functions of vertical and rotational displacements, as well as resonant frequencies for the first and second modes, have been investigated.

The MIKROMASH HQNSC15 probe has been used as the silicon rectangular AFM cantilever with a silicon tip. The dimensional and material parameters of the cantilever were: length L=130 μ m, width b=37 μ m, thickness h=3.59 μ m, mass density p=2330kg/m^3, Young's modulus E=1.5×10^11 Pa, Poisson's ratio v=0.28, tip radius R=10nm, Quality Factor Q₁=Q₂=100. A proportional damping was assumed with a uniform modal ξ =1/2Q. We set α =15^o and H=15 μ m. The polystyrene, polypropylene, polycarbonate, acrylonitrile butadiene styrene, and high-impact polystyrene polymers were chosen as the soft specimens. An increase in specimen elasticity raises the resonant frequency and reduces the magnitude of the FRF of vertical displacement.

In this study, the experimental methods were evaluated using a JPK AFM and a NanoWizard [9]. The polystyrene, polypropylene, polycarbonate, acrylonitrile butadiene styrene, and high-impact polystyrene polymers were chosen as the soft specimens. According to Tables 1 to 6 and Figures 10 to 15, an increase in specimen elasticity raises the resonant frequency and reduces the magnitude of the FRF of vertical displacement. Totally, the resonant frequency for extended strokes was greater than that of retraction strokes due to the greater Young's modulus for extended strokes. In this study,

the experimental methods were performed using JPK AFM and NanoWizard 3. Figures 8 and 14, along with Table 4, present the resonant frequencies of the cantilever in vacuum, evaluated through both theoretical and experimental methods [10]. Figure 5 illustrates that increasing the fluid viscosity reduces the resonant frequency and magnitude of the FRF due to an increase in the fluid damping coefficient. Figures 12 to 15 and Tables 1 and 4 display the excellent agreement between the resonant frequencies of the beam in water and methanol, as determined by both theoretical and experimental works [9].

Table 2. Resonant frequencies for AFM cantilever in water and supposing of diverse polymeric samples

Nanofiber format	First Frequency	Second Frequency
PS/extend	198943.67	1138753.61
PS/retract	194169.03	1137957.84
PS (exp)	188,429.8	992,396.7
HIPS/extend	187007.05	1136366.29
HIPS/retract	183823.95	1135570.51
HIPS (exp)	182,053.5	1,116,575
PP/extend	185415.5	1136366.29
PP/retract	183028.18	1135570.51
PP (exp)	182,715.2	1,237,748
ABS/extend	194169.03	1137957.84
ABS/retract	190190.15	1137162.06
ABS (Exp)	184,462.8	1,350,744
PC/Extend	192577.48	1137957.84
PC/Retract	189394.38	1137162.06
PC (exp)	188,429.8	960,991.7

Table 3. Residuum among resonant frequencies for AFM cantilever in water and supposing of diverse polymeric samples by FEM and experimental techniques

Specimens and indentation First frequency Second			
frequency methods			
PS (exp vs. extend)	5.28%	12.85%	
PS (exp vs. retract)	2.95%	12.79%	
HIPS (Exp vs. extend)	2.64%	1.74%	
HIPS (Exp vs. retract)	0.96%	1.67%	
PP (exp vs. extend)	1.45%	8.19%	
PP (exp vs. retract)	0.17%	8.25%	
ABS (exp vs. extend)	4.99%	15.75%	
ABS (exp vs. retract)	3.01%	15.81%	
PC (exp vs. extend)	2.15%	15.55%	
PC (exp vs. retract)	0.5%	15.49%	

Table 4. Resonant frequencies for AFM cantilever in methanol and supposing of diverse polymeric samples

Specimens and	First frequency	Second frequency	
indentation methods			
PS/extend	214859.17	1219126.86	
PS/retract	210084.52	1218331.08	
PS (exp)	211,438	1,252,348	
HIPS/extend	202922.55	1216739.53	
HIPS/retract	198943.67	1215943.76	
HIPS (exp)	200,975.5	1,155,132	
PP/extend	200535.22	1215943.76	
PP/retract	198147.9	1215943.76	
PP (exp)	198,476.8	1,291,325	
ABS/extend	210084.52	1218331.08	
ABS/retract	206105.65	1217535.31	
ABS (exp)	202,710.7	1,213,851	
PC/extend	208492.97	1218331.08	
PC/retract	204514.1	1216739.53	
PC (exp)	202,520.4	1,166,510	

Table 5. Residuum among resonant frequencies for AFM cantilever in methanol and supposing of diverse polymeric samples by FEM and experimental techniques

Specimens and indentation	First frequency	Second
methods		frequency
PS (exp vs. extend)	1.59%	2.65%
PS (exp vs. retract)	0.64%	2.71%
HIPS (exp vs. extend)	1.25%	5.06%
HIPS (exp vs. retract)	1.01%	5.01%
PP (exp vs. extend)	1.02%	5.83%
PP (exp vs. retract)	0.16%	5.83%
ABS (exp vs. extend)	3.5%	0.36%
ABS (exp vs. retract)	1.64%	0.3%
PC (exp vs. extend)	2.86%	4.25%
PC (exp vs. retract)	0.97%	4.12%

Table 6. Resonant frequencies for AFM cantilever in acetone and supposing of diverse polymeric samples

_			
Specimens and	First frequency	Second frequency	
indentation methods	1 0		
PS/extend	218042.27	1227084.6	
PS/retract	213267.62	1226288.83	
HIPS/extend	205309.87	1224697.28	
HIPS/retract	202126.77	1223901.5	
PP/extend	203718.32	1223901.5	
PP/retract	201331.	1223901.5	
ABS/extend	213267.62	1226288.83	
ABS/retract	209288.75	1225493.06	
PC/extend	211676.07	1226288.83	
PC/retract	207697.2	1225493.06	

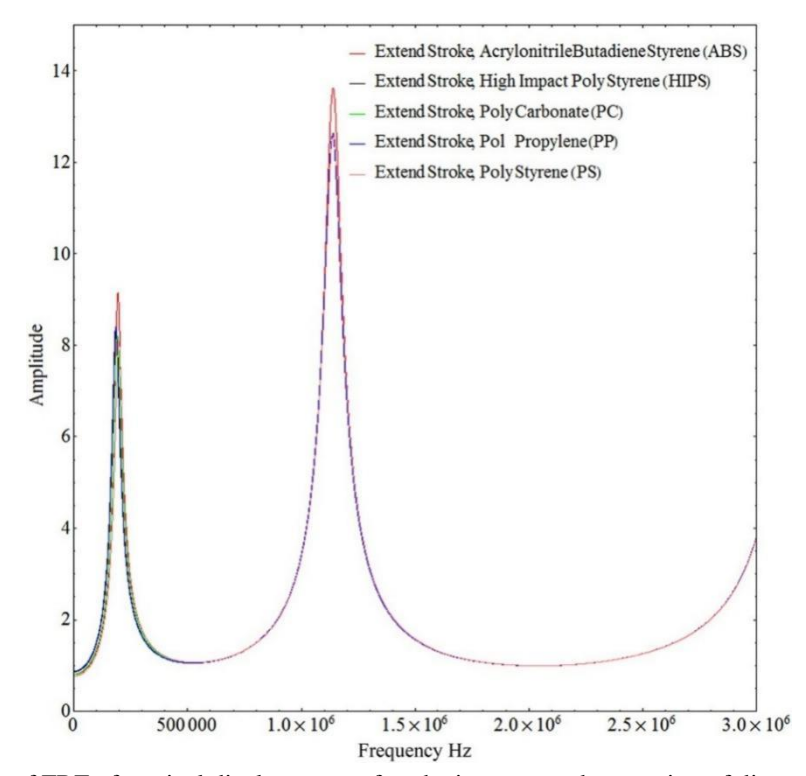


Figure 10. Amplitude of FRF of vertical displacement of probe in water and supposing of diverse polymeric specimens

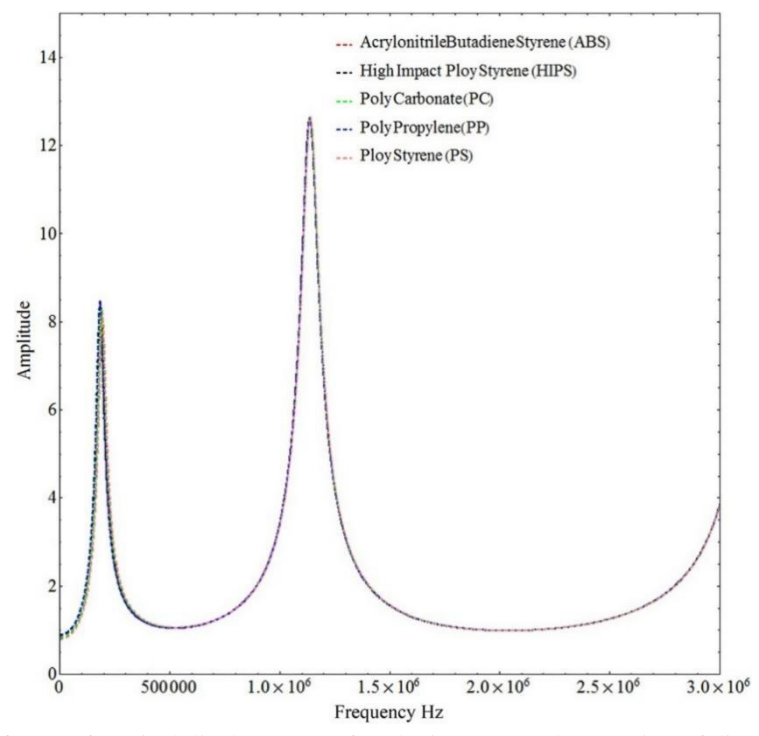


Figure 11. Amplitude of FRF of vertical displacement of probe in water and supposing of diverse polymeric specimens

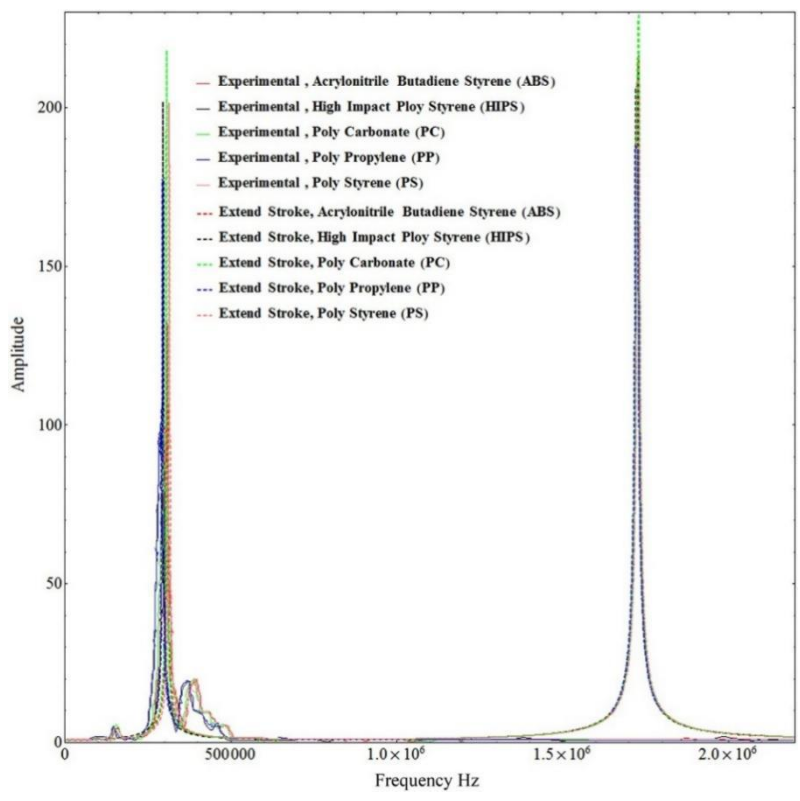


Figure 12. Amplitude of FRF of vertical displacement of probe in air by FEM and experimental methods and supposing of diverse polymeric specimens

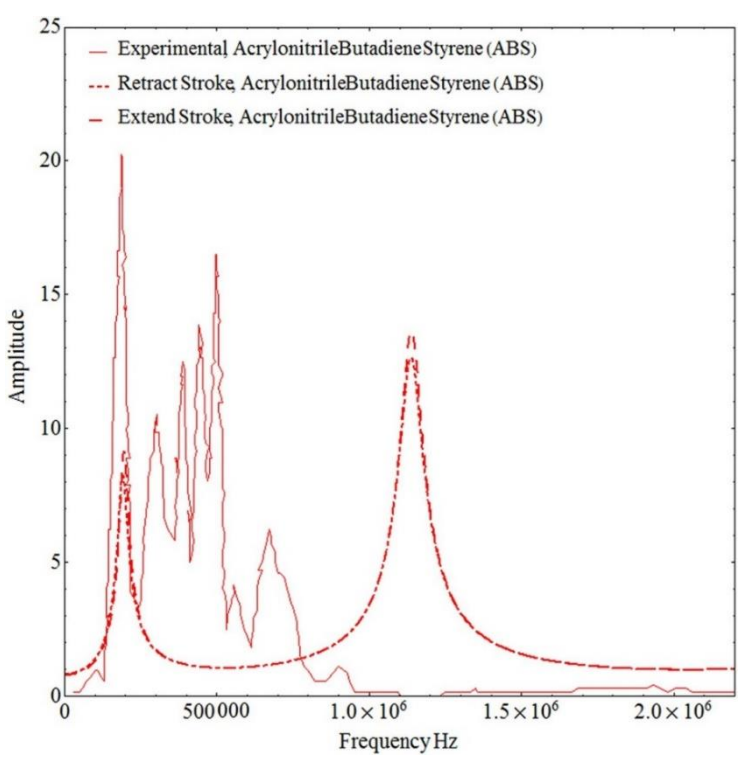


Figure 13. Amplitude of FRF of vertical displacement of probe in water by FEM and experimental methods and supposing acrylonitrile butadiene styrene (ABS) as the specimen

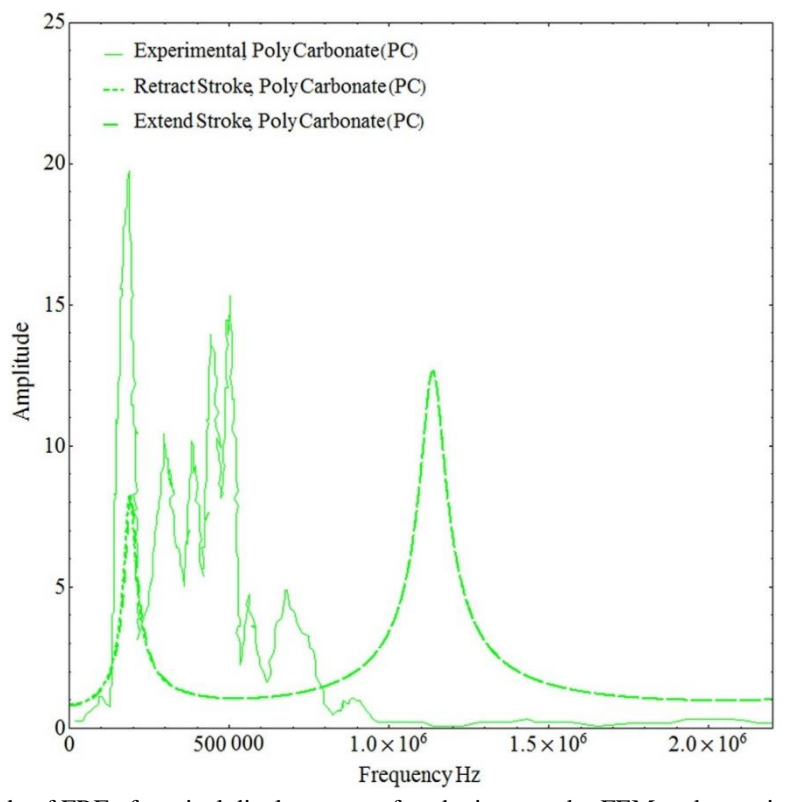


Figure 14. Amplitude of FRF of vertical displacement of probe in water by FEM and experimental methods and supposing polycarbonate (PC) as the specimen

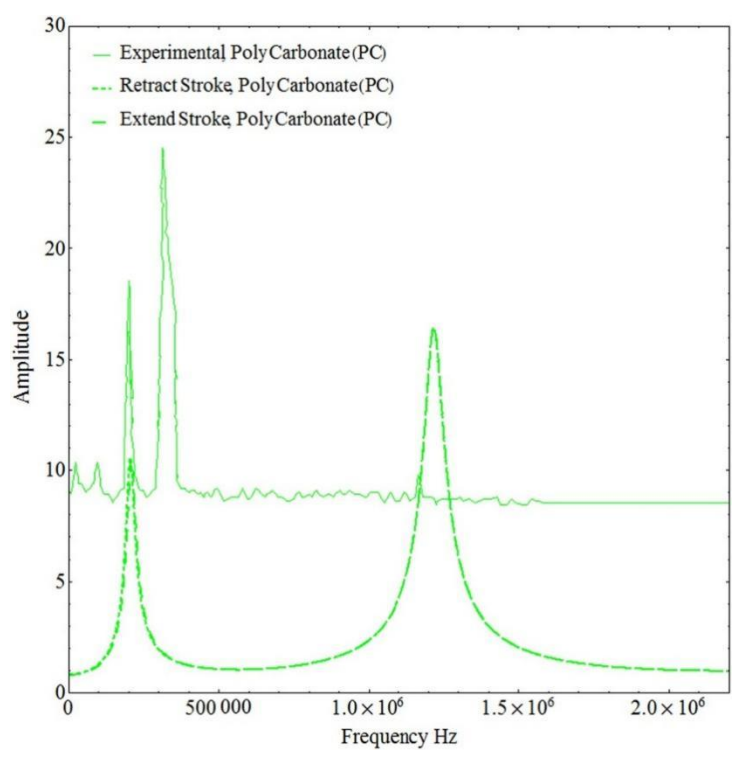


Figure 15. Amplitude of FRF of vertical displacement of probe in methanol by FEM and experimental methods and supposing polycarbonate (PC) as the specimen

7. Conclusions

In this study, the mechanical properties of soft materials, including five polymers, have been investigated using nanoindentation by AFM. Polystyrene (PS), polypropylene (PP), polycarbonate (PC), polyethylene (PE), acrylonitrile butadiene styrene (ABS), and high-impact polystyrene (HIPS) have been considered as the samples. Initially, the elastic modulus of the polymers was obtained using the NT-MDT SOLVER P47 scanning probe microscope for both extension and retraction strokes. The results show that an increase in elastic modulus increases the resonant frequency but decreases the amplitude of the FRF of vertical movement of the beam.

The results showed that the adhesion for the retraction stroke was larger than that for the extension stroke, which was attributed to the breakage of chemical bonds in the sample during the extension stroke.

The vibrational behavior of the V-shaped AFM beam, considering different polymers as samples and various immersion environments, has been investigated. Polystyrene (PS), polypropylene (PP), polycarbonate (PC), polyethylene (PE), acrylonitrile butadiene styrene (ABS), and high-impact polystyrene (HIPS) have been considered as the samples. Air, water, methanol, and acetone have been considered as immersion media. Initially, the elastic modulus of the polymers was obtained using the NT-MDT SOLVER P47 scanning probe microscope for both extension and retraction strokes.

The results show that an increase in elastic modulus increases the resonant frequency but decreases the amplitude of the FRF of vertical movement of the beam. By decreasing the liquid viscosity, the resonant frequency and amplitude of the FRF of vertical movement of the beam increase.

The results obtained from FEM modeling of the V-shaped AFM beam have been compared with those from an experimental method using a JPK Instruments-NanoWizard 2 Atomic Force Microscope in both air and water as the ambient. The results show excellent agreement. Applying other contact theories, such as the Johnson, Kendall, and Roberts (JKR) or Lennard–Jones contact theories, for modeling the tip–sample interaction force, and utilizing other theories to model the hydrodynamic force due to the liquid environment, is suggested for future work.

Recently, various functional biomaterials, including silk fibroin, poly-L-lactic acid (PLLA), and polycaprolactone (PCL), have been introduced. Studying the mechanical properties of these new biomaterials is suggested for future work.

8. References

- [1] Binning, G., Rohere, H., Gerber, C. and Weibel, E. 1983. Surface Studies by Scanning Tunneling Microscopy. Physical Review Letters. 49(1):57-61. doi:10.1103/PhysRevLett.49.57.
- [2] Gholizade Pasha, A. and Sadeghi, A. 2020. Non-Linear Vibrations of Immersed Dagger Shaped Atomic Force Microscope Cantilever in Different Liquids by Experimental and Theoretical Methods. Journal of Applied Mechanics and Technical Physics. 61 (4):652-660. doi:10.1134/S0021894420040197.
- [3] Gholizade Pasha, A. and Sadeghi, A. 2020. Experimental and theoretical investigations about the nonlinear vibrations of rectangular atomic force microscope cantilevers immersed in different liquids. Archive of Applied Mechanics. 90 (9):1893-1917. doi:10.1007/s00419-020-01703-5.
- [4] Gholizade Pasha, A. and Sadeghi, A. 2020. A fresh study for dynamic behaviour of atomic force microscope cantilever by considering different immersion environment. Journal of Experimental Nanoscience. 15(1):129-149. doi:10.1080/17458080.2020.1754398.
- [5] Binning, G., Quate, C.F. and Gerber, C. 1986. Atomic Force Microscope. Physical Review Letters. 56(9):930-933. doi:10.1103/PhysRevLett.56.930.
- [6] Hurley, D. C., Shen, K., Jennett, N. M. and Turner J.A. 2003. atomic force acoustic microscopy methods to determine thin-film elastic properties. J. Appl. Phys. 94:2347-2354. doi:10.1063/1.1592632.
- [7] Dupas, E., Gremaud, G. and Kulik, A. 2001. High-Frequency Mechanical Spectroscopy with an Atomic Force Microscope. Review of Scientific Instruments. 72(10). doi:10.1063/1.1403009.
- [8] Sadeghi, A. 2013. A new Investigation for Double Tapered Atomic Force Microscope Cantilevers by Considering the Damping Effect. ZAMM Journal of Applied Mathematics and Mechanics. 3(95):283-296. doi:10.1002/zamm.201200268.
- [9] Gholizade, Pasha, A. and Sadeghi, A. 2021. A new insight into the vibrational modeling of contact mode for atomic force microscope beams in various immersion ambiances. Microscopy Research and Technique. 84 (4):771-781. doi.org/10.1002/jemt.23635.
- [10] Gholizade, Pasha, A. and Sadeghi, A. 2020. Experimental and theoretical studies of frequency response function of dagger-shaped atomic force microscope in different immersion environments. Journal of Microscopy. 279 (1):52-68. doi:10.1111/jmi.12897.